Demonstrating Agreement between Radio and Fluorescence Measurements of the Depth of Maximum of Extensive Air Showers at the Pierre Auger Observatory

A. Abdul Halim,[13] P. Abreu,[73] M. Aglietta,[55,53] I. Allekotte,[1] K. Almeida Cheminant,[71] A. Almela,[7,12] R. Aloisio,[46,47] J. Alvarez-Muñiz,[79] J. Ammerman Yebra,[79] G. A. Anastasi,[55,53] L. Anchordoqui,[86] B. Andrada,[7] S. Andringa,[73] Anukriti,[76] L. Apollonio,[60,50] C. Aramo,[51] P. R. Araújo Ferreira,[43] E. Arnone,[64,53] J. C. Arteaga Velázquez,[68] P. Assis,[73] G. Avila,[11] E. Avocone,[58,47] A. Bakalova,[33] F. Barbato,[46,47] A. Bartz Mocellin,[85] J. A. Bellido,[13,70] C. Berat,[37] M. E. Bertaina,[64,53] G. Bhatta,[71] M. Bianciotto,[64,53] P. L. Biermann,[i] V. Binet,[5] K. Bismark,[40,7] T. Bister,[80,81] J. Biteau,[38,b] J. Blazek,[33] C. Bleve,[37] J. Blümer,[42] M. Boháčová,[33] D. Boncioli,[58,47] C. Bonifazi,[8,27] L. Bonneau Arbeletche,[22] N. Borodai,[71] J. Brack,[k] P. G. Brichetto Orchera,[7] F. L. Briechle,[43] A. Bueno,[78] S. Buitink,[15] M. Buscemi,[48,62] M. Büsken,[40,7] A. Bwembya,[80,81] K. S. Caballero-Mora,[67] S. Cabana-Freire,[79] L. Caccianiga,[60,50] R. Caruso,[59,48] A. Castellina,[55,53] F. Catalani,[19] G. Cataldi,[49] L. Cazon,[79] M. Cerda,[10] A. Cermenati,[46,47] J. A. Chinellato,[22] J. Chudoba,[33] L. Chytka,[34] R. W. Clay,[13] A. C. Cobos Cerutti,[6] R. Colalillo,[61,51] A. Coleman,[90] M. R. Coluccia,[49] R. Conceição,[73] A. Condorelli,[38] G. Consolati,[50,56] M. Conte,[57,49] F. Convenga,[58,47] D. Correia dos Santos,[29] P. J. Costa,[73] C. E. Covault,[84] M. Cristinziani,[45] C. S. Cruz Sanchez,[3] S. Dasso,[4,2] K. Daumiller,[42] B. R. Dawson,[13] R. M. de Almeida,[29] J. de Jesús,[7,42] S. J. de Jong,[80,81] J. R. T. de Mello Neto,[27,28] I. De Mitri,[46,47] J. de Oliveira,[18] D. de Oliveira Franco,[22] F. de Palma,[57,49] V. de Souza,[20] B. P. de Souza de Errico,[27] E. De Vito,[57,49] A. Del Popolo,[59,48] O. Deligny,[35] N. Denner,[33] L. Deval,[42,7] A. di Matteo,[53] M. Dobre,[74] C. Dobrigkeit,[22] J. C. D'Olivo,[69] L. M. Domingues Mendes,[73] Q. Dorosti,[45] J. C. dos Anjos,[16] R. C. dos Anjos,[26] J. Ebr,[33] F. Ellwanger,[42] M. Emam,[80,81] R. Engel,[40,42] I. Epicoco,[57,49] M. Erdmann,[43] A. Etchegoyen,[7,12] C. Evoli,[46,47] H. Falcke,[80,82,81] J. Farmer,[89] G. Farrar,[88] A. C. Fauth,[22] N. Fazzini,[f] F. Feldbusch,[41] F. Fenu,[42,e] A. Fernandes,[73] B. Fick,[87] J. M. Figueira,[7] A. Filipčič,[77,76] T. Fitoussi,[42] B. Flaggs,[90] T. Fodran,[80] T. Fujii,[89,g] A. Fuster,[7,12] C. Galea,[80] C. Galelli,[60,50] B. García,[6] C. Gaudu,[39] H. Gemmeke,[41] F. Gesualdi,[7,42] A. Gherghel-Lascu,[74] P. L. Ghia,[35] U. Giaccari,[49] J. Glombitza,[43,h] F. Gobbi,[10] F. Gollan,[7] G. Golup,[1] M. Gómez Berisso,[1] P. F. Gómez Vitale,[11] J. P. Gongora,[11] J. M. González,[1] N. González,[7] I. Goos,[1] D. Góra,[71] A. Gorgi,[55,53] M. Gottowik,[79] T. D. Grubb,[13] F. Guarino,[61,51] G. P. Guedes,[23] E. Guido,[45] L. Gülzow,[42] S. Hahn,[40] P. Hamal,[33] M. R. Hampel,[7] P. Hansen,[3] D. Harari,[1] V. M. Harvey,[13] A. Haungs,[42] T. Hebbeker,[43] C. Hojvat,[f] J. R. Hörandel,[80,81] P. Horvath,[34] M. Hrabovský,[34] T. Huege,[42,15] A. Insolia,[59,48] P. G. Isar,[75] P. Janecek,[33] V. Jilek,[33] J. A. Johnsen,[85] J. Jurysek,[33] K.-H. Kampert,[39] B. Keilhauer,[42] A. Khakurdikar,[80] V. V. Kizakke Covilakam,[7,42] H. O. Klages,[42] M. Kleifges,[41] F. Knapp,[40] J. Köhler,[42] N. Kunka,[41] B. L. Lago,[17] N. Langner,[43] M. A. Leigui de Oliveira,[25] Y. Lema-Capeans,[79] A. Letessier-Selvon,[36] I. Lhenry-Yvon,[35] L. Lopes,[73] L. Lu,[91] Q. Luce,[40] J. P. Lundquist,[76] A. Machado Payeras,[22] M. Majercakova,[33] D. Mandat,[33] B. C. Manning,[13] P. Mantsch,[f] S. Marafico,[35] F. M. Mariani,[60,50] A. G. Mariazzi,[3] I. C. Mariş,[14] G. Marsella,[62,48] D. Martello,[57,49] S. Martinelli,[42,7] O. Martínez Bravo,[65] M. A. Martins,[79] H.-J. Mathes,[42] J. Matthews,[a] G. Matthiae,[63,52] E. Mayotte,[85,39] S. Mayotte,[85] P. O. Mazur,[f] G. Medina-Tanco,[69] J. Meinert,[39] D. Melo,[7] A. Menshikov,[41] C. Merx,[42] S. Michal,[34] M. I. Micheletti,[5] L. Miramonti,[60,50] S. Mollerach,[1] F. Montanet,[37] L. Morejon,[39] C. Morello,[55,53] K. Mulrey,[80,81] R. Mussa,[53] W. M. Namasaka,[39] S. Negi,[33] L. Nellen,[69] K. Nguyen,[87] G. Nicora,[9] M. Niechciol,[45] D. Nitz,[87] D. Nosek,[32] V. Novotny,[32] L. Nožka,[34] A. Nucita,[57,49] L. A. Núñez,[31] C. Oliveira,[20] M. Palatka,[33] J. Pallotta,[9] S. Panja,[33] G. Parente,[79] T. Paulsen,[39] J. Pawlowsky,[39] M. Pech,[33] J. Pękala,[71] R. Pelayo,[66] L. A. S. Pereira,[24] E. E. Pereira Martins,[40,7] J. Perez Armand,[21] C. Pérez Bertolli,[7,42] L. Perrone,[57,49] S. Petrera,[46,47] C. Petrucci,[58,47] T. Pierog,[42] M. Pimenta,[73] M. Platino,[7] B. Pont,[80] M. Pothast,[81,80] M. Pourmohammad Shahvar,[62,48] P. Privitera,[89] M. Prouza,[33] A. Puyleart,[87] S. Querchfeld,[39] J. Rautenberg,[39] D. Ravignani,[7] J. V. Reginatto Akim,[22] M. Reininghaus,[40] J. Ridky,[33] F. Riehn,[79] M. Risse,[45] V. Rizi,[58,47] W. Rodrigues de Carvalho,[80] E. Rodriguez,[7,42] J. Rodriguez Rojo,[11] M. J. Roncoroni,[7] S. Rossoni,[44] M. Roth,[42] E. Roulet,[1] A. C. Rovero,[4] P. Ruehl,[45] A. Saftoiu,[74] M. Saharan,[80] F. Salamida,[58,47] H. Salazar,[65] G. Salina,[52] J. D. Sanabria Gomez,[31] F. Sánchez,[7] E. M. Santos,[21] E. Santos,[33] F. Sarazin,[85] R. Sarmento,[73] R. Sato,[11] P. Savina,[91] C. M. Schäfer,[40] V. Scherini,[57,49] H. Schieler,[42] M. Schimassek,[35] M. Schimp,[39] D. Schmidt,[42] O. Scholten,[15,j] H. Schoorlemmer,[80,81] P. Schovánek,[33] F. G. Schröder,[90,42] J. Schulte,[43] T. Schulz,[42] S. J. Sciutto,[3] M. Scornavacche,[7,42] A. Segreto,[54,48] S. Sehgal,[39] S. U. Shivashankara,[76] G. Sigl,[44] G. Silli,[7] O. Sima,[74,c] K. Simkova,[15] F. Simon,[41] R. Smau,[74] R. Šmída,[89] P. Sommers,[l] J. F. Soriano,[86] R. Squartini,[10] M. Stadelmaier,[50,60,42] S. Stanič,[76] J. Stasielak,[71] P. Stassi,[37] S. Strähnz,[40] M. Straub,[43] T. Suomijärvi,[38] A. D. Supanitsky,[7] Z. Svozilikova,[33] Z. Szadkowski,[72] F. Tairli,[13] A. Tapia,[30] C. Taricco,[64,53] C. Timmermans,[81,80] O. Tkachenko,[42] P. Tobiska,[33] C. J. Todero Peixoto,[19] B. Tomé,[73] Z. Torrès,[37]

A. Travaini,[10] P. Travnicek,[33] C. Trimarelli,[58,47] M. Tueros,[3] M. Unger,[42] L. Vaclavek,[34] M. Vacula,[34] J. F. Valdés Galicia,[69] L. Valore,[61,51] E. Varela,[65] A. Vásquez-Ramírez,[31] D. Veberič,[42] C. Ventura,[28] I. D. Vergara Quispe,[3] V. Verzi,[52] J. Vicha,[33] J. Vink,[83] S. Vorobiov,[76] C. Watanabe,[27] A. A. Watson,[d] A. Weindl,[42] L. Wiencke,[85] H. Wilczyński,[71] D. Wittkowski,[39] B. Wundheiler,[7] B. Yue,[39] A. Yushkov,[33] O. Zapparrata,[14] E. Zas,[79] D. Zavrtanik,[76,77] and M. Zavrtanik[77,76]

(Pierre Auger Collaboration)

[1]*Centro Atómico Bariloche and Instituto Balseiro (CNEA-UNCuyo-CONICET), San Carlos de Bariloche, Argentina*
[2]*Departamento de Física and Departamento de Ciencias de la Atmósfera y los Océanos, FCEyN, Universidad de Buenos Aires and CONICET, Buenos Aires, Argentina*
[3]*IFLP, Universidad Nacional de La Plata and CONICET, La Plata, Argentina*
[4]*Instituto de Astronomía y Física del Espacio (IAFE, CONICET-UBA), Buenos Aires, Argentina*
[5]*Instituto de Física de Rosario (IFIR)—CONICET/U.N.R. and Facultad de Ciencias Bioquímicas y Farmacéuticas U.N.R., Rosario, Argentina*
[6]*Instituto de Tecnologías en Detección y Astropartículas (CNEA, CONICET, UNSAM), and Universidad Tecnológica Nacional—Facultad Regional Mendoza (CONICET/CNEA), Mendoza, Argentina*
[7]*Instituto de Tecnologías en Detección y Astropartículas (CNEA, CONICET, UNSAM), Buenos Aires, Argentina*
[8]*International Center of Advanced Studies and Instituto de Ciencias Físicas, ECyT-UNSAM and CONICET, Campus Miguelete—San Martín, Buenos Aires, Argentina*
[9]*Laboratorio Atmósfera—Departamento de Investigaciones en Láseres y sus Aplicaciones—UNIDEF (CITEDEF-CONICET), Argentina*
[10]*Observatorio Pierre Auger, Malargüe, Argentina*
[11]*Observatorio Pierre Auger and Comisión Nacional de Energía Atómica, Malargüe, Argentina*
[12]*Universidad Tecnológica Nacional—Facultad Regional Buenos Aires, Buenos Aires, Argentina*
[13]*University of Adelaide, Adelaide, South Australia, Australia*
[14]*Université Libre de Bruxelles (ULB), Brussels, Belgium*
[15]*Vrije Universiteit Brussels, Brussels, Belgium*
[16]*Centro Brasileiro de Pesquisas Fisicas, Rio de Janeiro, Rio de Janeiro, Brazil*
[17]*Centro Federal de Educação Tecnológica Celso Suckow da Fonseca, Petropolis, Brazil*
[18]*Instituto Federal de Educação, Ciência e Tecnologia do Rio de Janeiro (IFRJ), Brazil*
[19]*Universidade de São Paulo, Escola de Engenharia de Lorena, Lorena, São Paulo, Brazil*
[20]*Universidade de São Paulo, Instituto de Física de São Carlos, São Carlos, São Paulo, Brazil*
[21]*Universidade de São Paulo, Instituto de Física, São Paulo, São Paulo, Brazil*
[22]*Universidade Estadual de Campinas, IFGW, Campinas, São Paulo, Brazil*
[23]*Universidade Estadual de Feira de Santana, Feira de Santana, Brazil*
[24]*Universidade Federal de Campina Grande, Centro de Ciencias e Tecnologia, Campina Grande, Brazil*
[25]*Universidade Federal do ABC, Santo André, São Paulo, Brazil*
[26]*Universidade Federal do Paraná, Setor Palotina, Palotina, Brazil*
[27]*Universidade Federal do Rio de Janeiro, Instituto de Física, Rio de Janeiro, Rio de Janeiro, Brazil*
[28]*Universidade Federal do Rio de Janeiro (UFRJ), Observatório do Valongo, Rio de Janeiro, Rio de Janeiro, Brazil*
[29]*Universidade Federal Fluminense, EEIMVR, Volta Redonda, Rio de Janeiro, Brazil*
[30]*Universidad de Medellín, Medellín, Colombia*
[31]*Universidad Industrial de Santander, Bucaramanga, Colombia*
[32]*Charles University, Faculty of Mathematics and Physics, Institute of Particle and Nuclear Physics, Prague, Czech Republic*
[33]*Institute of Physics of the Czech Academy of Sciences, Prague, Czech Republic*
[34]*Palacky University, Olomouc, Czech Republic*
[35]*CNRS/IN2P3, IJCLab, Université Paris-Saclay, Orsay, France*
[36]*Laboratoire de Physique Nucléaire et de Hautes Energies (LPNHE), Sorbonne Université, Université de Paris, CNRS-IN2P3, Paris, France*
[37]*Université Grenoble Alpes, CNRS, Grenoble Institute of Engineering Université Grenoble Alpes, LPSC-IN2P3, 38000 Grenoble, France*
[38]*Université Paris-Saclay, CNRS/IN2P3, IJCLab, Orsay, France*
[39]*Bergische Universität Wuppertal, Department of Physics, Wuppertal, Germany*
[40]*Karlsruhe Institute of Technology (KIT), Institute for Experimental Particle Physics, Karlsruhe, Germany*
[41]*Karlsruhe Institute of Technology (KIT), Institut für Prozessdatenverarbeitung und Elektronik, Karlsruhe, Germany*

[42]Karlsruhe Institute of Technology (KIT), Institute for Astroparticle Physics, Karlsruhe, Germany
[43]RWTH Aachen University, III. Physikalisches Institut A, Aachen, Germany
[44]Universität Hamburg, II. Institut für Theoretische Physik, Hamburg, Germany
[45]Universität Siegen, Department Physik—Experimentelle Teilchenphysik, Siegen, Germany
[46]Gran Sasso Science Institute, L'Aquila, Italy
[47]INFN Laboratori Nazionali del Gran Sasso, Assergi (L'Aquila), Italy
[48]INFN, Sezione di Catania, Catania, Italy
[49]INFN, Sezione di Lecce, Lecce, Italy
[50]INFN, Sezione di Milano, Milano, Italy
[51]INFN, Sezione di Napoli, Napoli, Italy
[52]INFN, Sezione di Roma "Tor Vergata," Roma, Italy
[53]INFN, Sezione di Torino, Torino, Italy
[54]Istituto di Astrofisica Spaziale e Fisica Cosmica di Palermo (INAF), Palermo, Italy
[55]Osservatorio Astrofisico di Torino (INAF), Torino, Italy
[56]Politecnico di Milano, Dipartimento di Scienze e Tecnologie Aerospaziali, Milano, Italy
[57]Università del Salento, Dipartimento di Matematica e Fisica "E. De Giorgi," Lecce, Italy
[58]Università dell'Aquila, Dipartimento di Scienze Fisiche e Chimiche, L'Aquila, Italy
[59]Università di Catania, Dipartimento di Fisica e Astronomia "Ettore Majorana," Catania, Italy
[60]Università di Milano, Dipartimento di Fisica, Milano, Italy
[61]Università di Napoli "Federico II," Dipartimento di Fisica "Ettore Pancini," Napoli, Italy
[62]Università di Palermo, Dipartimento di Fisica e Chimica "E. Segrè," Palermo, Italy
[63]Università di Roma "Tor Vergata," Dipartimento di Fisica, Roma, Italy
[64]Università Torino, Dipartimento di Fisica, Torino, Italy
[65]Benemérita Universidad Autónoma de Puebla, Puebla, México
[66]Unidad Profesional Interdisciplinaria en Ingeniería y Tecnologías Avanzadas del Instituto Politécnico Nacional (UPIITA-IPN), México, Distrito Federal, México
[67]Universidad Autónoma de Chiapas, Tuxtla Gutiérrez, Chiapas, México
[68]Universidad Michoacana de San Nicolás de Hidalgo, Morelia, Michoacán, México
[69]Universidad Nacional Autónoma de México, México, Distrito Federal, México
[70]Universidad Nacional de San Agustin de Arequipa, Facultad de Ciencias Naturales y Formales, Arequipa, Peru
[71]Institute of Nuclear Physics PAN, Krakow, Poland
[72]University of Łódź, Faculty of High-Energy Astrophysics,Łódź, Poland
[73]Laboratório de Instrumentação e Física Experimental de Partículas—LIP and Instituto Superior Técnico—IST, Universidade de Lisboa—UL, Lisboa, Portugal
[74]"Horia Hulubei" National Institute for Physics and Nuclear Engineering, Bucharest-Magurele, Romania
[75]Institute of Space Science, Bucharest-Magurele, Romania
[76]Center for Astrophysics and Cosmology (CAC), University of Nova Gorica, Nova Gorica, Slovenia
[77]Experimental Particle Physics Department, J. Stefan Institute, Ljubljana, Slovenia
[78]Universidad de Granada and C.A.F.P.E., Granada, Spain
[79]Instituto Galego de Física de Altas Enerxías (IGFAE), Universidade de Santiago de Compostela, Santiago de Compostela, Spain
[80]IMAPP, Radboud University Nijmegen, Nijmegen, The Netherlands
[81]Nationaal Instituut voor Kernfysica en Hoge Energie Fysica (NIKHEF), Science Park, Amsterdam, The Netherlands
[82]Stichting Astronomisch Onderzoek in Nederland (ASTRON), Dwingeloo, The Netherlands
[83]Universiteit van Amsterdam, Faculty of Science, Amsterdam, The Netherlands
[84]Case Western Reserve University, Cleveland, Ohio, USA
[85]Colorado School of Mines, Golden, Colorado, USA
[86]Department of Physics and Astronomy, Lehman College, City University of New York, Bronx, New York, USA
[87]Michigan Technological University, Houghton, Michigan, USA
[88]New York University, New York, New York, USA
[89]University of Chicago, Enrico Fermi Institute, Chicago, Illinois, USA
[90]University of Delaware, Department of Physics and Astronomy, Bartol Research Institute, Newark, Delaware, USA
[91]University of Wisconsin-Madison, Department of Physics and WIPAC, Madison, Wisconsin, USA

(Received 30 March 2023; revised 16 October 2023; accepted 24 October 2023; published 8 January 2024)

We show, for the first time, radio measurements of the depth of shower maximum (X_{max}) of air showers induced by cosmic rays that are compared to measurements of the established fluorescence method at the same location. Using measurements at the Pierre Auger Observatory we show full compatibility between our radio and the previously published fluorescence dataset, and between a subset of air showers observed simultaneously with both radio and fluorescence techniques, a measurement setup unique to the Pierre Auger Observatory. Furthermore, we show radio X_{max} resolution as a function of energy and demonstrate the ability to make competitive high-resolution X_{max} measurements with even a sparse radio array. With this, we show that the radio technique is capable of cosmic-ray mass composition studies, both at Auger and at other experiments.

DOI: 10.1103/PhysRevLett.132.021001

The origin and nature of cosmic rays has been one of the driving questions in astroparticle physics in the past century. Especially for ultrahigh energy cosmic rays, much remains to be discovered about their sources, their acceleration mechanisms, and how they propagate. A particularly important range of cosmic-ray energies to investigate is the so-called transition region. There the sources of cosmic rays are expected to transition from Galactic to extragalactic origin, which is commonly expected to occur in the energy range between 10^{17} and 10^{19} eV [1]. Current efforts in this regime focus on measuring the cosmic-ray flux, the arrival direction, and the composition of cosmic-ray primaries. Of these, mass composition is particularly important to distinguish between different possible source models.

The Pierre Auger Observatory [2] in Argentina, covering 3000 km^2, is the largest facility dedicated to detecting ultrahigh-energy cosmic rays (UHECRs). The primary components are an array of 1660 water-Cherenkov detectors, also called the surface detector (SD) and 27 fluorescence telescopes, known as the fluorescence detector (FD), that overlook the SD. The observatory also has an array of radio detectors, the Auger Engineering Radio Array (AERA) [3], located within the grid of the SD and close to one of the FD sites. AERA was constructed to measure the radio signals produced in extensive air showers at energies between 10^{17} and 10^{19} eV. It thus probes the transition region with independent and complementary measurements to those made with fluorescence light, air-Cherenkov light, and secondary particles of air showers. The technique of radio detection of cosmic rays has made great steps in the past twenty years providing understanding of the emission mechanisms, the implementation in simulation codes, and the reconstruction of shower properties [4–10] (see also [11–13] for extensive reviews).

Radio emission in air showers is produced by time-varying currents from the movement of electrons and positrons. These arise from acceleration in the magnetic field of the Earth and ionization of the atmosphere while the shower develops. The currents give rise to electromagnetic radiation at frequencies, predominantly, in the MHz to GHz regime that arrives on the ground as a short pulse of a few nanoseconds. The frequency spectrum and spatial distribution are governed by the fact that the source moves relativistically in a medium with a refractive index gradient, which leads to a Cherenkov-like time compression. By sampling the radio-emission footprint over an extended area with an array of radio antennas, one can reconstruct the properties of the air shower and derive information about the primary cosmic ray. For example, the arrival direction of the cosmic ray can be reconstructed based on the arrival times of the signals in multiple antennas and the strength of the radio emission footprint scales with the energy of the air shower [10,13,14]. The general shape of the footprint also changes with the particle type of the primary cosmic ray. This is because a heavier primary particle (e.g., an iron nucleus) essentially behaves like a superposition of lower-energy protons that interact earlier in the atmosphere than a single proton with all the energy. The heavier particle will thus produce a wider radio emission footprint on the ground. Therefore, the shape of the footprint is a mass-sensitive probe for the primary particle type. We don't directly observe the particle type, but it is strongly related to the atmospheric depth X where the shower is maximally developed, the depth of the shower maximum X_{max}, which we can observe. Hence, X_{max} is used as the main probe in this work to investigate the types of particles inducing the air-shower signals measured by AERA.

In this work we present the results of a technique to measure X_{max}, developed for AERA, using data measured over seven years. We compare this to measurements from the FD to show compatibility and, in addition, perform a direct comparison of X_{max} of showers measured simultaneously by both detectors. Next, we evaluate the resolution of the method to demonstrate the competitiveness of the radio method. Finally, we compare these results to other experiments and discuss the implications.

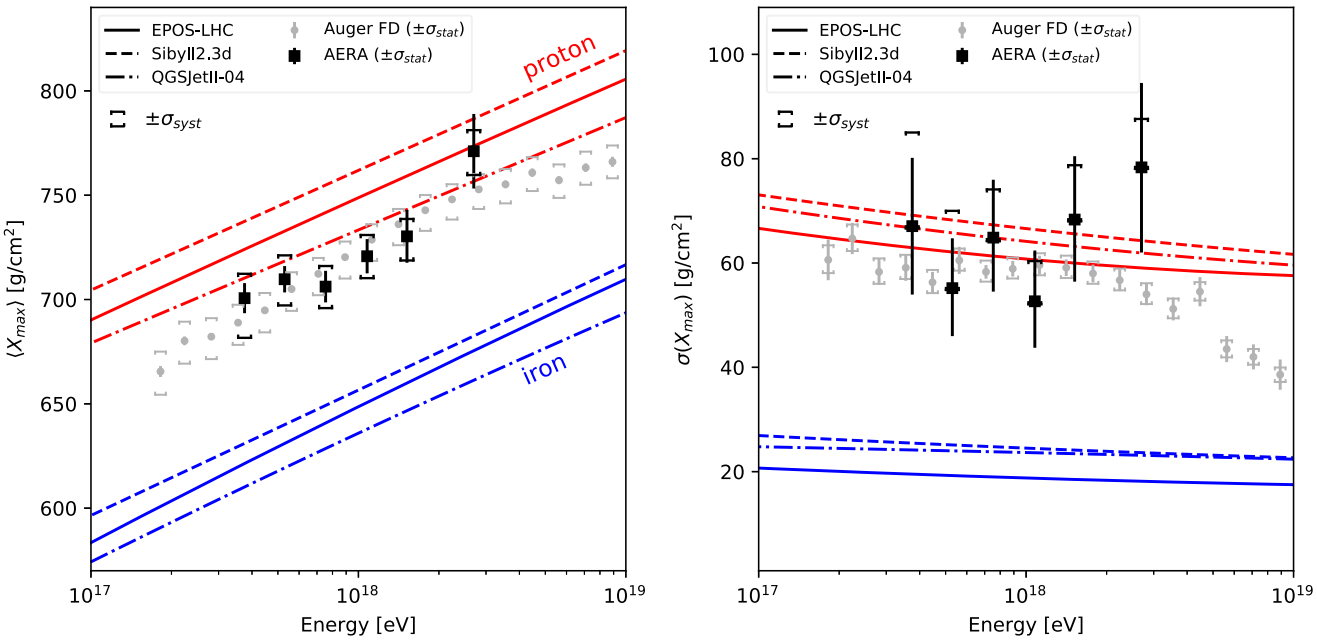

FIG. 1. Mean (left) and standard deviation (right) of the $X_{\max}$ distribution as measured by AERA in this work (black). The results are compared to predictions from CORSIKA air-shower simulations for three hadronic interaction models (lines) for proton (red) and iron (blue) mass compositions [15–18] and compared to measurements by the Auger FD [18]. The statistical uncertainties on the mean and width of the measurements are plotted as error bars and the systematic uncertainties with capped markers.

The $X_{\max}$ distribution.—In Fig. 1 we show the first two central moments of the distributions of reconstructed $X_{\max}$ values (as a function of the SD energy [19]) resulting from 594 measured air showers. For this, we have used the state-of-the-art air-shower simulation code (CORSIKA v7.7100 [20] with radio extension CoREAS [8]) to generate an ensemble of 27 simulated air showers for each of our measured air showers. To achieve the highest precision possible we use a model of the atmosphere [21,22] and geomagnetic field [23] at the time and location of each shower. These simulations are generated such that they cover the $X_{\max}$ phase space. We then compare the measured radio signals to the simulated signals to derive the $X_{\max}$ value that best represents the measurements. Details on the reconstruction method, which builds upon [24,25], are presented in an accompanying publication [26]. The 594 showers have been selected to have energies above $E = 10^{17.5}$ eV, the threshold for full efficiency of the SD particle trigger [27,28], and to be detectable by AERA for any realistically occurring $X_{\max}$ value (i.e., an acceptance cut for radio) [26]. With the results, we demonstrate that the AERA measurements of the first and second moment of the $X_{\max}$ distribution (black markers) are compatible with the measurements of the fluorescence telescopes at the Pierre Auger Observatory (gray markers). Note that while for $\langle X_{\max}\rangle$ a mixed composition will result in values in between the lines for a pure proton and a pure iron composition, a mixed composition can result in $\sigma(X_{\max})$ values even larger than those of a pure proton composition. The statistical agreement of the results of AERA and the FD provides independent support for the validity of the FD measurements [18] and shows that the radio method is able to perform the same measurements. It also confirms the validity of the microscopic radio-emission simulations of CoREAS. The comparison of radio and fluorescence measurements might also provide a way in the future to improve constraints on the systematic uncertainties of the fluorescence method. For example, by lowering the uncertainties on atmospheric corrections.

Direct comparison with hybrid radio-fluorescence measurements.—We can also make a direct comparison between the two $X_{\max}$ reconstruction techniques at Auger, using a subset of 53 air showers (predominantly between $10^{17.5}$ and 10^{18} eV), that were measured simultaneously by both the FD and AERA. When comparing the $X_{\max}$ values on an event-by-event basis (Fig. 2) we find an average difference of $\langle X_{\max}^{\mathrm{AERA}} - X_{\max}^{\mathrm{FD}}\rangle = -3.9 \pm 11.2\ \mathrm{g\,cm^{-2}}$, demonstrating there to be no significant bias. The distribution of the differences is compatible with a Gaussian distribution with the combined $X_{\max}$ resolution of our method and the FD ($53.3 \pm 5.7\ \mathrm{g\,cm^{-2}}$ versus the distribution width of $58.8 \pm 5.8\ \mathrm{g\,cm^{-2}}$). Additionally, the average difference shows no significant change when applying, for example, cuts on energy or $X_{\max}$ resolution, indicating this set of hybrid showers is well behaved. The average difference further strengthens the agreement between the fluorescence and radio methods as it shows agreement not just on the mean $X_{\max}$ versus energy between two datasets, but also on an event-to-event level where the effects of event-selection bias are absent.

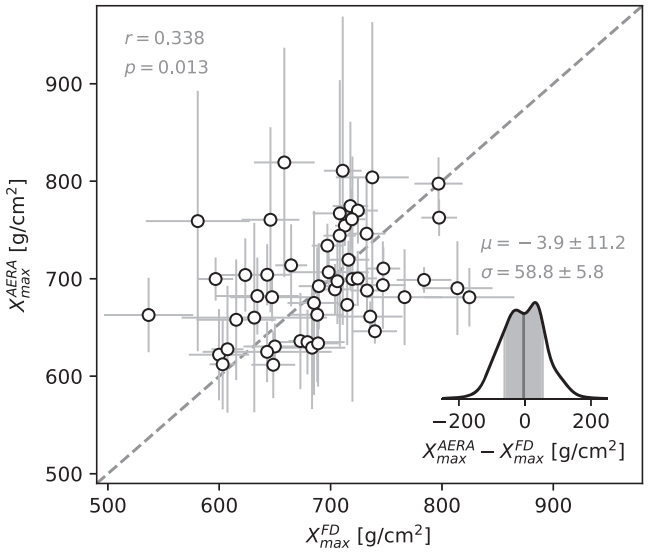

FIG. 2. Comparison of $X_{\max}$ for showers measured simultaneously by both AERA and the FD. A diagonal line is shown to guide the eye. Shown at the top is the Pearson correlation coefficient r with corresponding p value (the probability to obtain an r of at least that value from uncorrelated data). Shown at the bottom is the distribution (kernel density estimation) of the differences with mean μ and spread σ.

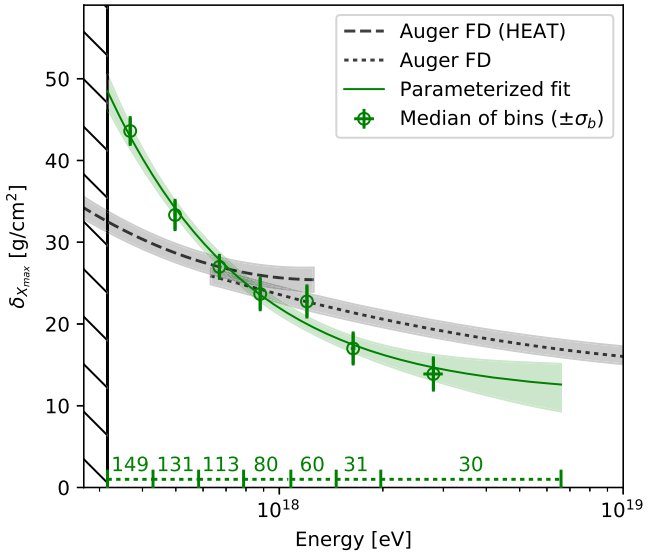

FIG. 3. Resolution of the $X_{\max}$ reconstruction method, $\delta_{X_{\max}}$, as a function of energy in units of column density. The median values of the uncertainties on $X_{\max}$ (circles with uncertainties σ_b from bootstrap resampling) for our set of showers are shown per energy bin along with the parametrized fit [Eq. (1)] of the resolution of $X_{\max}$ (solid line with 1σ-confidence bands). Also shown are the resolutions achieved by the Auger fluorescence telescopes [29]. The black hatched region at low energy indicates the cut on energy for this AERA analysis. The size of the energy bins with the number of showers per bin is inset at the bottom of the figure.

Furthermore, the agreement between the two methods directly illustrates that both the FD and radio $X_{\max}$ reconstructions are well understood. The fluorescence method involves imaging the trajectory of the air shower. When one accounts for the attenuation of the light one can extract the depth in the atmosphere where the fluorescence emission is strongest, corresponding to $X_{\max}$. The radio technique in contrast is not affected by attenuation, yet other effects play a role. The coherence of the radio signal is a key factor as it strongly affects what we observe in our antennas. Thus, the spatial distribution of particles in the shower down to the scales set by our highest frequency (80 MHz, corresponding to 3.75 m) is directly probed. Furthermore, the radio emission is the result of two emission mechanisms that interfere with each other (arising from time-varying transverse and longitudinal currents) and it is in addition affected by the refractive index gradient of the atmosphere. Because of this complexity, we have used air-shower simulations to obtain $X_{\max}$ by comparing the measured and simulated radio signals in our antennas. So, when we are comparing the $X_{\max}$ measurements of the two techniques, we not only test that all of these effects are accounted for correctly, but we inherently also test the implementation of the radio-emission calculation in simulations (both the simulation of the electromagnetic cascade as well as the radio emission in a discretized classical electrodynamics calculation). The agreement on $X_{\max}$ by AERA and the FD thus strongly suggests that all of these aspects are well under control.

The $X_{\max}$ resolution.—We determined an uncertainty for each reconstructed $X_{\max}$ value based on the reconstruction of simulated showers, allowing us to directly evaluate the resolution of our method. In Fig. 3 we show the median $X_{\max}$ resolution versus cosmic-ray energy E (green points), demonstrating that we are able to reach a resolution of better than 15 g cm^{-2} at the highest energies (13.9 ± 2.0 g cm^{-2} for the last bin). Towards lower energies, the resolution becomes worse, mainly because of the weaker radio signals at lower energies (leading to lower signal-to-noise ratios in our antennas). For comparison we also show the resolution obtained by the fluorescence telescopes at the Pierre Auger Observatory [29], demonstrating the competitiveness of the radio technique over a wide energy range. Because of the large set of showers, we are also able to evaluate the energy dependence of the $X_{\max}$ resolution. We parameterize our resolution $\delta_{X_{\max}}$ as a function of energy (green line) inspired by the energy resolution of electromagnetic calorimeters [30] and similar to the shapes used for the FD:

$$\delta_{X_{\max}} = a \cdot \sqrt{\frac{10^{18}\ \text{eV}}{E}} \oplus b \cdot \frac{10^{18}\ \text{eV}}{E} \oplus c, \qquad (1)$$

where $a = 14.0 \pm 6.8$ g cm^{-2}, $b = 12.7 \pm 2.5$ g cm^{-2}, and $c = 11.2 \pm 4.7$ g cm^{-2} are free parameters, and

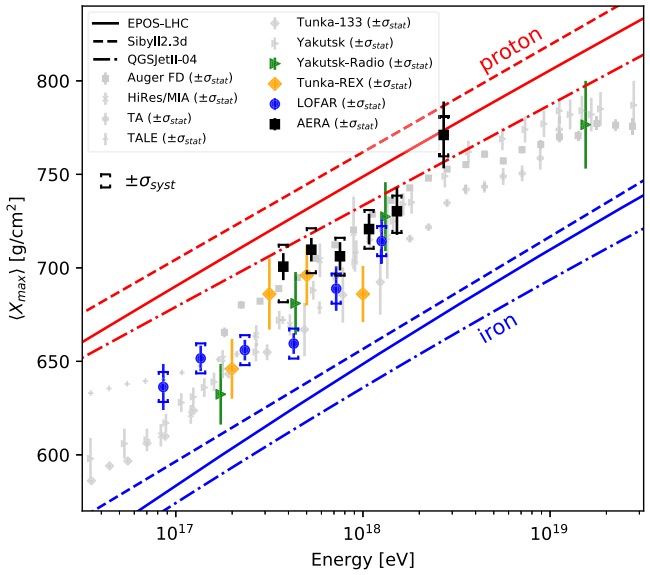

FIG. 4. Mean of the $X_{\max}$ distribution as measured by AERA in this work (black). The results are compared to predictions from air-shower simulations for multiple hadronic interaction models (lines) for proton (red) and iron (blue) mass compositions [15–18] and compared to measurements by LOFAR [31], Tunka-Rex [33], Yakutsk-Radio [34], and Auger FD [18]. Note that the Yakutsk-Radio results do not account for aperture effects on the same level as the other experiments. Colors have been used to highlight the measurements with the radio technique. The statistical uncertainties on the measurements are shown as vertical bars and for radio the systematic uncertainties, if available, are shown with caps.

$\oplus$ indicates the quadratic sum. The c parameter provides a prediction of the potential resolution that our method might be able to reach for AERA data. For radio experiments with a denser antenna spacing or experiments with lower ambient noise conditions one might reasonably expect this resolution to be even better. For example, LOFAR reported an average resolution of 19 g cm^{-2} using a similar method [31] and simulation studies for the upcoming Square Kilometer Array suggest an average resolution of 6–8 g cm^{-2} could be reached [32]. In all likelihood their respective resolutions will improve with energy similar to the trend shown for AERA, making the radio technique very competitive for precision $X_{\max}$ measurements.

Comparison to other experiments.—In Fig. 4 we show our $\langle X_{\max}\rangle$ results together with various results from previous works. Measurements by other experiments that use the radio technique to measure $X_{\max}$ are highlighted in color. In the past, Tunka-Rex [33], Yakutsk-Radio [34], and LOFAR [31] (and its prototype LOPES [35]) have shown $X_{\max}$ measurements, but it has been challenging to make significant statements on the compatibility of the radio technique with fluorescence and air-Cherenkov light measurements. This is because these experiments either didn't have a second technique to directly compare to or due to a combination of large statistical uncertainties and limited investigation of detector-specific systematic uncertainties. It is difficult to make statements on the compatibility of AERA and Tunka-Rex or Yakutsk-Radio without a full picture of those systematic uncertainties, but there do not seem to be significant discrepancies within their statistical uncertainties (note that the highest energy bin of Tunka-Rex only contains ten showers, hence its deviation with AERA is arguably not significant). However, the LOFAR measurements include a detailed estimation of systematic uncertainties, have much smaller statistical uncertainties than Tunka-Rex or Yakutsk-Radio, and share many similarities with AERA in the method to reconstruct $X_{\max}$, so we can compare these results to the FD and AERA results.

We note that the difference between the Auger FD and LOFAR measurements, as can be seen in Fig. 4, previously left open the possibility of a systematic shift in $X_{\max}$ due to an inherent difference between radio and fluorescence techniques. However, the AERA $X_{\max}$ results now show no significant bias with respect to the fluorescence results, not when comparing their full datasets nor on an event-to-event level. Additionally, a study of the compatibility of the full shape of the $X_{\max}$ distribution as measured by AERA and the Auger FD, available in [26], also finds no significant discrepancies within uncertainties. This strongly suggests that the differences between Auger and LOFAR must be either physical (e.g., due to differences in the magnetic field or atmospheric conditions, their altitudes, or their southern versus northern exposure) or systematic (e.g., due to the event selection or reconstruction), but not inherent to either the radio or fluorescence techniques.

At higher energies, a seemingly similar difference in $\langle X_{\max}\rangle$ (both in magnitude and direction) can be observed between the fluorescence results of Auger (gray squares) and TA (gray plus markers). However, a detailed comparison by an Auger-TA working group has found that, given the known selection bias in the TA data, this difference is compatible within uncertainties [36]. This comparison only covers energies above $10^{18.2}$ eV, so does not overlap with the LOFAR data. An AERA-LOFAR working group has started looking into their apparent differences, investigating, for example, differences in event selection, $X_{\max}$ reconstruction method, and energy scale. Regardless, a deeper comparison of AERA and LOFAR data opens a new way to try to understand and reduce systematic uncertainties on air-shower and cosmic-ray parameters. Furthermore, the combination of fluorescence and radio measurements, linked by hybrid detectors such as at Auger, might resolve or constrain differences even more.

Conclusions.—In this work, we have used seven years of AERA data to investigate the depth of maximum of extensive air showers at energies where the cosmic-ray origin is expected to transition from Galactic to extragalactic sources. We show our $X_{\max}$ results to be in agreement with the results of the fluorescence telescopes at the Pierre

Auger Observatory. In addition, this compatibility is also demonstrated on an event-by-event level with simultaneous radio and fluorescence measurements of the same air showers. With our method, we are able to achieve competitive high-resolution $X_{\max}$ reconstructions, reaching resolutions near 15 $\mathrm{g\,cm^{-2}}$ at the highest energies. With this, we have demonstrated that the reconstruction of $X_{\max}$ at AERA is both well understood and competitive with established methods, and ready to be used in future experiments.

The successful installation, commissioning, and operation of the Pierre Auger Observatory would not have been possible without the strong commitment and effort from the technical and administrative staff in Malargüe. We are very grateful to the following agencies and organizations for financial support: Argentina—Comisión Nacional de Energía Atómica; Agencia Nacional de Promoción Científica y Tecnológica (ANPCyT); Consejo Nacional de Investigaciones Científicas y Técnicas (CONICET); Gobierno de la Provincia de Mendoza; Municipalidad de Malargüe; NDM Holdings and Valle Las Leñas; in gratitude for their continuing cooperation over land access; Australia—the Australian Research Council; Belgium—Fonds de la Recherche Scientifique (FNRS); Research Foundation Flanders (FWO), Marie Curie Action of the European Union Grant No. 101107047; Brazil—Conselho Nacional de Desenvolvimento Científico e Tecnológico (CNPq); Financiadora de Estudos e Projetos (FINEP); Fundação de Amparo à Pesquisa do Estado de Rio de Janeiro (FAPERJ); São Paulo Research Foundation (FAPESP) Grants No. 2019/10151-2, No. 2010/07359-6, and No. 1999/05404-3; Ministério da Ciência, Tecnologia, Inovações e Comunicações (MCTIC); Czech Republic—Grants No. MSMT CR LTT18004, No. LM2015038, No. LM2018102, No. LM2023032, No. CZ.02.1.01/0.0/0.0/16_013/0001402, No. CZ.02.1.01/0.0/0.0/18_046/0016010, and No. CZ.02.1.01/0.0/0.0/17_049/0008422; France—Centre de Calcul IN2P3/CNRS; Centre National de la Recherche Scientifique (CNRS); Conseil Régional Ile-de-France; Département Physique Nucléaire et Corpusculaire (PNC-IN2P3/CNRS); Département Sciences de l'Univers (SDU-INSU/CNRS); Institut Lagrange de Paris (ILP) Grant No. LABEX ANR-10-LABX-63 within the Investissements d'Avenir Programme Grant No. ANR-11-IDEX-0004-02; Germany—Bundesministerium für Bildung und Forschung (BMBF); Deutsche Forschungsgemeinschaft (DFG); Finanzministerium Baden-Württemberg; Helmholtz Alliance for Astroparticle Physics (HAP); Helmholtz-Gemeinschaft Deutscher Forschungszentren (HGF); Ministerium für Kultur und Wissenschaft des Landes Nordrhein-Westfalen; Ministerium für Wissenschaft, Forschung und Kunst des Landes Baden-Württemberg; Italy—Istituto Nazionale di Fisica Nucleare (INFN); Istituto Nazionale di Astrofisica (INAF); Ministero dell'Università e della Ricerca (MUR); CETEMPS Center of Excellence; Ministero degli Affari Esteri (MAE), ICSC Centro Nazionale di Ricerca in High Performance Computing, Big Data and Quantum Computing, funded by European Union NextGenerationEU, reference code CN_00000013; México—Consejo Nacional de Ciencia y Tecnología (CONACYT) No. 167733; Universidad Nacional Autónoma de México (UNAM); PAPIIT DGAPA-UNAM; The Netherlands—Ministry of Education, Culture and Science; Netherlands Organisation for Scientific Research (NWO); Dutch national e-infrastructure with the support of SURF Cooperative; Poland—Ministry of Education and Science, Grants No. DIR/WK/2018/11 and No. 2022/WK/12; National Science Centre, Grants No. 2016/22/M/ST9/00198, No. 2016/23/B/ST9/01635, No. 2020/39/B/ST9/01398, and No. 2022/45/B/ST9/02163; Portugal—Portuguese national funds and FEDER funds within Programa Operacional Factores de Competitividade through Fundação para a Ciência e a Tecnologia (COMPETE); Romania—Ministry of Research, Innovation and Digitization, National Research Council-Executive Agency for Higher Education, Research, Development and Innovation Funding (CNCS-UEFISCDI), Contract No. 30N/2023 under Romanian National Core Program LAPLAS VII, Grant No. PN 23 21 01 02 and Project No. PN-III-P1-1.1-TE-2021-0924/TE57/2022, within PNCDI III; Slovenia—Slovenian Research Agency, Grants No. P1-0031, No. P1-0385, No. I0-0033, No. N1-0111; Spain—Ministerio de Economía, Industria y Competitividad (FPA2017-85114-P and PID2019–104676 GB-C32), Xunta de Galicia (ED431C 2017/07), Junta de Andalucía (SOMM17/6104/UGR, P18-FR-4314) Feder Funds, RENATA Red Nacional Temática de Astropartículas (FPA2015-68783-REDT) and María de Maeztu Unit of Excellence (MDM-2016-0692); USA—Department of Energy, Contracts No. DE-AC02-07CH11359, No. DE-FR02-04ER41300, No. DE-FG02-99ER41107, and No. DE-SC0011689; National Science Foundation, Grant No. 0450696; The Grainger Foundation; Marie Curie-International Research Staff Exchange Scheme/European Particle physics Latin America NETwork; European Particle Physics Latin American Network; and UNESCO.

[a]Present address: Louisiana State University, Baton Rouge, Los Angeles, USA.
[b]Also at Institut universitaire de France (IUF), France.
[c]Also at University of Bucharest, Physics Department, Bucharest, Romania.
[d]Present address: School of Physics and Astronomy, University of Leeds, Leeds, United Kingdom.
[e]Present address: Agenzia Spaziale Italiana (ASI). Via del Politecnico 00133, Roma, Italy.

[f]Present address: Fermi National Accelerator Laboratory, Fermilab, Batavia, Illinois, USA.
[g]Present address: Graduate School of Science, Osaka Metropolitan University, Osaka, Japan.
[h]Present address: ECAP, Erlangen, Germany.
[i]Present address: Max-Planck-Institut für Radioastronomie, Bonn, Germany.
[j]Also at Kapteyn Institute, University of Groningen, Groningen, The Netherlands.
[k]Present address: Colorado State University, Fort Collins, Colorado, USA.
[l]Present address: Pennsylvania State University, University Park, Pennsylvania, USA.

[1] A. Coleman *et al.*, Astropart. Phys. **149**, 102819 (2023).
[2] A. Aab *et al.* (Pierre Auger Collaboration), Nucl. Instrum. Methods Phys. Res., Sect. A **798**, 172 (2015).
[3] P. Abreu *et al.* (Pierre Auger Collaboration), J. Instrum. **7**, P10011 (2012).
[4] H. Falcke *et al.* (LOPES Collaboration), Nature (London) **435**, 313 (2005).
[5] O. Scholten, K. Werner, and F. Rusydi, Astropart. Phys. **29**, 94 (2008).
[6] D. Ardouin *et al.*, Astropart. Phys. **31**, 192 (2009).
[7] J. Alvarez-Muniz, W. R. Carvalho, Jr., and E. Zas, Astropart. Phys. **35**, 325 (2012).
[8] T. Huege, M. Ludwig, and C. W. James, AIP Conf. Proc. **1535**, 128 (2013).
[9] A. Nelles *et al.*, J. Cosmol. Astropart. Phys. 05 (2015) 018.
[10] A. Aab *et al.*, Phys. Rev. Lett. **116**, 241101 (2016).
[11] T. Huege, Phys. Rep. **620**, 1 (2016).
[12] F. G. Schröder, Prog. Part. Nucl. Phys. **93**, 1 (2017).
[13] F. G. Schröder *et al.*, EPJ Web Conf. **283**, 01001 (2023).
[14] A. Aab *et al.*, Phys. Rev. D **93**, 122005 (2016).
[15] S. Ostapchenko, Nucl. Phys. B, Proc. Suppl. **151**, 143 (2006).
[16] T. Pierog, Iu. Karpenko, J. M. Katzy, E. Yatsenko, and K. Werner, Phys. Rev. C **92**, 034906 (2015).
[17] F. Riehn, R. Engel, A. Fedynitch, T. K. Gaisser, and T. Stanev, Phys. Rev. D **102**, 063002 (2020).
[18] A. Yushkov *et al.* (Pierre Auger Collaboration), Proc. Sci. ICRC2019 (**2019**) 482.
[19] B. R. Dawson *et al.* (Pierre Auger Collaboration), Proc. Sci. ICRC2019 (**2019**) 231.
[20] D. Heck *et al.*, FZKA Tech. Umw. Wis. B **6019**, 1 (1998).
[21] P. Mitra *et al.*, Astropart. Phys. **123**, 102470 (2020).
[22] P. Abreu *et al.*, Astropart. Phys. **35**, 591 (2012).
[23] C. C. Finlay *et al.*, Geophys. J. Int. **183**, 1216 (2010).
[24] S. Buitink *et al.*, Nature (London) **531**, 70 (2016).
[25] S. Buitink *et al.*, Phys. Rev. D **90**, 082003 (2014).
[26] A. Abdul Halim *et al.* (Pierre Auger Collaboration), companion paper, Phys. Rev. D **109**, 022002 (2024).
[27] P. Abreu *et al.* (Pierre Auger Collaboration), Eur. Phys. J. C **81**, 966 (2021).
[28] D. Ravignani *et al.* (Pierre Auger Collaboration), in *Proceedings of the 33rd International Cosmic Ray Conference* (Brazilian Journal of Physics, Rio de Janeiro, 2013), 0693.
[29] J. Bellido *et al.* (Pierre Auger Collaboration), Proc. Sci. ICRC2017 (**2017**) 506.
[30] C. W. Fabjan and F. Gianotti, Rev. Mod. Phys. **75**, 1243 (2003).
[31] A. Corstanje *et al.*, Phys. Rev. D **103**, 102006 (2021).
[32] S. Buitink *et al.*, Proc. Sci. ICRC2021 (**2021**) 415.
[33] P. A. Bezyazeekov *et al.* (Tunka-Rex Collaboration), Phys. Rev. D **97**, 122004 (2018).
[34] I. Petrov and S. Knurenko, Proc. Sci. ICRC2019 (**2019**) 385.
[35] F. G. Schröder *et al.* (LOPES Collaboration), Proc. Sci. ICRC2017 (**2017**) 458.
[36] A. Yushkov *et al.* (Pierre Auger and Telescope Array Collaborations), Proc. Sci., ICRC2023 (**2023**) 249.